

# Battery-free RFID-enabled Wireless Sensors

Li Yang<sup>1</sup>, Giulia Orecchini<sup>2</sup>, George Shaker<sup>2,3</sup>, Ho-Seon Lee<sup>2</sup>, and Manos M. Tentzeris<sup>2</sup>

<sup>1</sup>Texas Instruments, Dallas, TX, 75243, U.S.A.

<sup>2</sup>Georgia Institute of Technology, Atlanta, GA, 30332, U.S.A.

<sup>3</sup>University of Waterloo, Waterloo, ON, Canada

*E-mail: li-yang@ti.com*

**Abstract** — This paper introduces the realization of batter-free RFID-enabled wireless sensors by integrating conformal RFID antennas with inkjet-printed carbon nanotubes (CNT) composites in a chipless RFID fashion for gas detection. The whole module is realized by inkjet printing on a low-cost paper-based substrate and the RFID tag is designed for the European UHF RFID band. The electrical conductivity of the CNT film changes in the presence of very small quantities of gases like ammonia, methanol, ethanol, acetone and nitrogen oxide (NO<sub>x</sub>), resulting in the variation of the backscattered power level which can be easily detected by the RFID reader to realize reliable wireless toxic gas sensing. The electrical performance characterization of the inkjet-printed CNT film is also reported in the UHF band.

**Index Terms** — Carbon nanotube composites, RFID, RFID-enabled sensor, UHF, RF passives, inkjet printing, gas sensing, wireless sensor

## I. INTRODUCTION

As the demand for low cost, flexible and power-efficient broadband wireless electronics increases, the materials and integration techniques become more and more critical and face more challenges, especially with the ever growing interest for “cognitive intelligence” and wireless applications, married with RFID technologies. This demand is further enhanced by the need for inexpensive, reliable, and durable wireless RFID-enabled sensor nodes that is driven by several applications, such as logistics, Aero-ID, anti-counterfeiting, supply-chain monitoring, space, healthcare, pharmaceutical, and is regarded as one of the most disruptive technologies to realize truly ubiquitous ad-hoc networks [1].

From the power consumption prospect, RFID-enabled sensors can be divided into two categories: active ones and passive ones. The active RFID-enabled sensor tags use batteries to power their communication circuitry, and benefit from relatively long wireless range. However, the need of external battery limits their applications to where battery replacements are only possible and affordable. Battery technology is mature, extensively commercialized, and completely self-contained. However, given current energy density and shelf-life trends, even for relatively large batteries and conservative communication schedules, the mean time to replacement is only a year or two. For some applications, such as harsh environment monitoring, in which battery changing is

not easy, the problem is aggravated significantly. Concerns over relatively short battery life have restricted wireless device applications.

Researchers have been looking for passive RFID-enabled sensor solutions. Some passive RFID prototypes for sensing applications have been proposed [2][3]. However, the sensing capabilities are usually realized by adding a discrete sensor or a special coating to the RFID tag, resulting in the difficulty in low-profile integration. Plus, the sensitivity is usually low. Therefore, there has been a growing interest in new materials in RFID sensing applications: an ultra sensitive composite which can be printed directly on the same substrate together with the antenna, for a low cost, flexible, highly integrated RFID module.

Carbon Nanotubes (CNT) composites have been found to have electrical conductance highly sensitive to extremely small quantities of gases, in addition to being compatible with inkjet-printing [4]. In this paper, a battery-free conformal CNT-based RFID-enabled sensor node for gas sensing applications, fully printed directly on paper substrate, is presented. Specifically, in this study, one benchmarking RFID tag was designed for the European UHF RFID band centering at 868 MHz. The printed CNT particles were Single-Walled Carbon Nanotubes (SWCNT) from Carbon Solutions, which were dispersed in dimethylformamide (DMF) solution and sonicated to meet the viscosity requirement for the inkjet printer. The impedance of the SWCNT film forms the sensor part. The antenna was printed first, followed by the layers of the dispersed SWCNT as a load. Thus in presence of a given gas, the resistance of the CNT will change resulting in a variation of the backscattered power from the RFID. This power level variation will be detected by the RFID reader to realize the gas detection. In experiment, when 4% consistency ammonia was imported into the gas chamber, the SWCNT impedance changed, resulting in a 10.8dB variation in the backscattered power from the tag antenna, that can be easily detected by the RFID reader to realize the “real-time” gas detection.

## II. INKJET-PRINTED SWCNT

CNT represents one of the most promising materials in the environmental sensor field since its discovery. To date, single-

walled CNT (SWNT) has attracted most extensive attention due to the relatively simple structures and easy prediction of properties by theoretical calculations. The geometrical structure of an SWNT can be seen as a cylindrical roll-up of a shingle sheet of graphene.

CNT has shown sensitivity towards extremely small quantities of gases. Due to the distortion of the electron clouds of CNT from a uniform distribution in graphite to asymmetric distribution around cylindrical nanotubes, a rich  $\pi$ -electron conjugation forms outside of the CNT, making it electrochemically active. The electrical properties of CNT are extremely sensitive to charge transfer and chemical doping effects by various molecules. When electron-withdrawing molecules (e.g.  $\text{NO}_2$ ) or electron-donating molecules (e.g.  $\text{NH}_3$ ) were absorbed by the semiconducting CNT, they will change the density of the main charge carriers of the nanotube, which changes the conductance of CNT. This behavior forms the basis for applications of CNT as electrical chemical gas sensors.

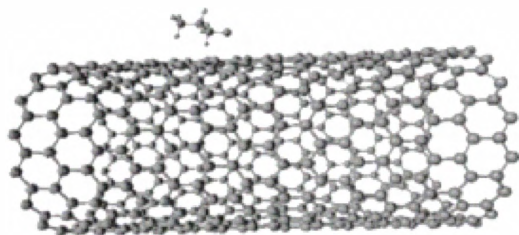


Fig. 1. Schematic geometry of SWNT with a molecule adsorbed on its external surface.

CNT composites have been found to be compatible with inkjet printing. As a direct-write technology, inkjet printing transfers the pattern directly to the substrate. Due to its capability of jetting one single ink droplet in an amount as low as 1 pl, it has widely drawn attention from the industrial world as a more accurate and economic fabrication method than the traditional lithography method. However, due to the insufficient molecular network formation among the inkjet-printed CNT particles at nano-scale, instabilities were observed in both the resistance and, especially, the reactance dependence on frequency above several MHz, which limits the CNT application in only DC or LF band [5]. To enable the CNT-enabled sensor to be integrated with RFID antenna at UHF band, a special recipe needs to be developed.

Two types of SWCNT, namely, P2-SWCNT and P3-SWCNT were tested. P2-SWCNT is developed from purified AP-SWNT by air oxidation and catalyst removing. P3-SWCNT is developed from AP-SWNT purified with nitric acid. Compared with P2-SWCNT, P3-SWCNT has much higher functionality and is easier to disperse in the solvent. In experiments, P2-SWCNT started to aggregate at the concentration lower than 0.1mg/ml, while P3-SWCNT can go up to 0.4mg/ml and still show good dispersion. Therefore, P3-

SWCNT was selected for the latter steps.

The sample SWCNT powder was dispersed in Dimethyl-Formamide (DMF), which is a polar aprotic solvent. The concentration of the ink was 0.4mg/ml. The diluted solution was purified by sonicated for 12 hours to prevent aggregations of large particle residues. This is important to avoid the nozzle clogging by SWCNT flocculation during the printing process. Dimatix Materials Printer DMP-2800 equipped with DMCLCP-11610 printer head was used to fire the SWCNT ink droplet onto a flexible substrate [6].

Silver electrodes were patterned with the nano-practical ink from Cabot before depositing the SWCNT film, followed by a sintering process. The electrode finger is 2mm by 10mm with a gap of 0.8mm. Then, the 3mm by 2mm SWCNT film was deposited. The 0.6mm overlapping zone is to ensure the good contact between the SWCNT film and the electrodes. Four devices with 10, 15, 20 and 25 SWCNT layers were fabricated to investigate the electrical properties. Fig. 2 shows the fabricated samples. The color depth of the SWCNT film is due to the different layers.

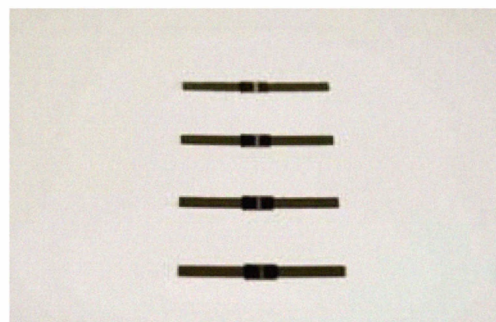


Fig. 2. Photograph of the inkjet-printed SWCNT films with silver electrodes. The SWCNT layers of the samples from up to down are 10, 15, 20 and 25, respectively.

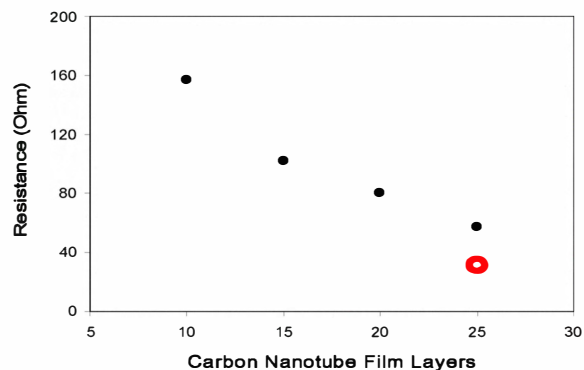


Fig. 3. Measured DC resistance of SWCNT gas sensors in air.

The electrical resistance of the device was measured by probing the end of the two electrodes. The DC resistance in air is shown in Fig. 3. As expected, the resistance goes down when the number of SWCNT layers increases. In fact, the resistance of the CNT layers can be decreased further by

changing the printer resolution. It has been observed that values can drop further down to 20 Ohms using a 1016 dpi setting, as marked by the red circle in Fig. 3.



Fig. 4. The setting of Tedlar bag gas chamber for SWCNT gas reaction.

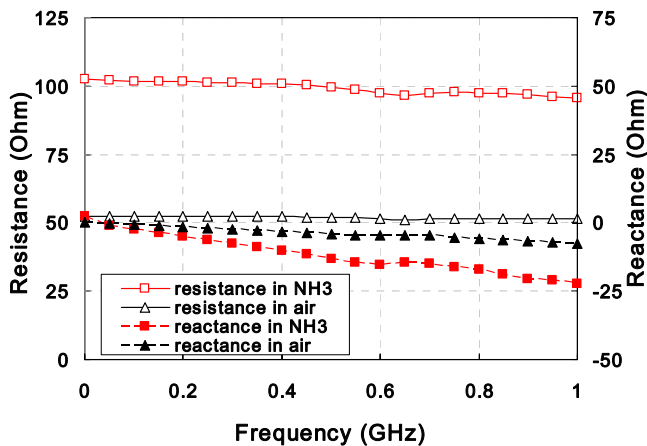


Fig. 5. Measured impedance characteristics of SWCNT film at UHF band.

To examine the CNT gas reaction performance, the DC resistance of a CNT strip was measured first in presence of ammonia and then in presence of ethanol, methanol and acetone. For example, the measured value of a 20-layer CNT strip in the first case increased from 80 to 100 Ohms, indicating CNT's sensing the presence of the gas. The other materials were in liquid state so they had to be evaporated in a container of known volume. For this purpose, a Tedlar bag of 20 liters volume is used as the gas chamber, as shown in Fig. 4. The liquid was placed in a Petri dish from which the known amount of the liquids was evaporated. The CNT strip was put inside the bag before the evaporation was started and once all of the liquid converted to a gaseous state, the DC resistance was measured. The values recorded were in the range of 100 to 200 Ohms depending on the concentrations of the gasses. Such variation demonstrates the potential of using CNT in sensing various gasses.

A network vector analyzer (Rohde&Schwarz ZVA8) was used to characterize the SWCNT film electrical performance

at UHF band before and after the gas reaction. A GS probe was placed on the silver electrodes for the impedance measurements. The calibration method used was short-open-load-thru (SOLT). In Fig. 5, the gas sensor of SWCNT composite shows a very stable impedance response up to 1GHz, which verifies the effectiveness of the developed SWCNT solvent recipe. At 868MHz, the 25-layer sensor exhibits a resistance of 51.6Ω and a reactance of -j6.1Ω in air. After meeting ammonia, the resistance was increased to 97.1Ω and the reactance was shifted to -j18.8Ω.

### III. RFID TAG MODULE

A passive RFID system operates in the following way: the RFID reader sends an interrogating RF signal to the RFID tag consisting of an antenna and an IC chip as a load. The IC responds to the reader by varying its input impedance, thus modulating the backscattered signal. The modulation scheme often used in RFID applications is amplitude shift keying (ASK) in which the IC impedance switches between the matched state and the mismatched state. The power reflection coefficient of the RFID antenna can be calculated as a measure to evaluate the reflected wave strength.

$$\eta = \left| \frac{Z_{Load} - Z_{ANT}^*}{Z_{Load} + Z_{ANT}} \right|^2 \quad (1)$$

where  $Z_{Load}$  represents the impedance of the load and  $Z_{ANT}$  represents the impedance of the antenna terminals with  $Z_{ANT}^*$  being its complex conjugate. The same mechanism can be used to realize RFID-enabled sensor modules. The SWCNT film functions as a tunable resistor  $Z_{Load}$  with a value determined by the existence of the target gas. The RFID reader monitors the backscattered power level. When the power level changes, it means that there is variation in the load impedance, therefore the sensor detects the existence of the gas.

Calculated from Friis free-space formula, the backscattered power received by the RFID reader is defined as

$$P_r = P_{ref} G_t G_r \eta \left( \frac{\lambda}{4\pi d} \right)^2 = P_t G_t^2 G_r^2 \eta \left( \frac{\lambda}{4\pi d} \right)^4 \quad (4)$$

or written in a decibel form, as

$$P_r = P_t + 2G_t + 2G_r - 40 \log_{10} \left( \frac{4\pi}{\lambda} \right) - 40 \log_{10}(d) + \eta \quad (5)$$

where  $P_t$  is the power fed into the reader antenna,  $G_t$  and  $G_r$  is the gain of the reader antenna and tag antenna, respectively, and  $d$  is the distance between the reader and the tag. In (5), except the term of  $\eta$ , all the other values remain constant before and after the RFID tag meets gas. Therefore the variation of the backscattered power level solely depends on  $\eta$ , which is determined by the impedance of the SWCNT film.

A bow-tie meander line dipole antenna was designed and

fabricated on a 100 $\mu$ m thickness flexible paper substrate with dielectric constant 3.2. The RFID prototype structure is shown in Fig. 6 along with dimensions, with the SWCNT film inkjet printed in the center. The nature of the bow-tie shape offers a more broadband operation for the dipole antenna.

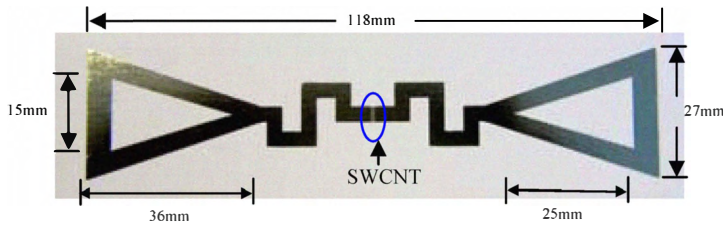


Fig. 6. The RFID tag module design on flexible substrate: (a) configuration (b) photograph of the tag with inkjet-printed SWCNT film as a load.

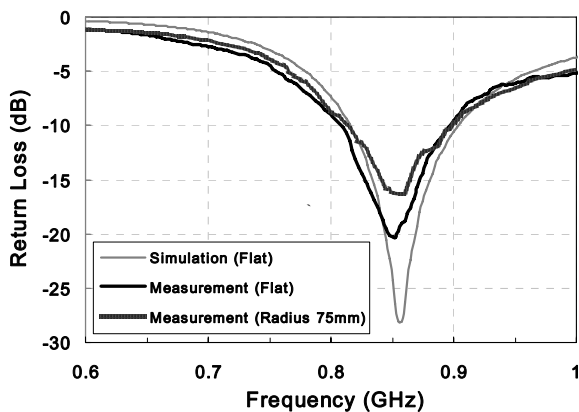


Fig. 7. Simulated and measured return loss of the RFID tag antenna.

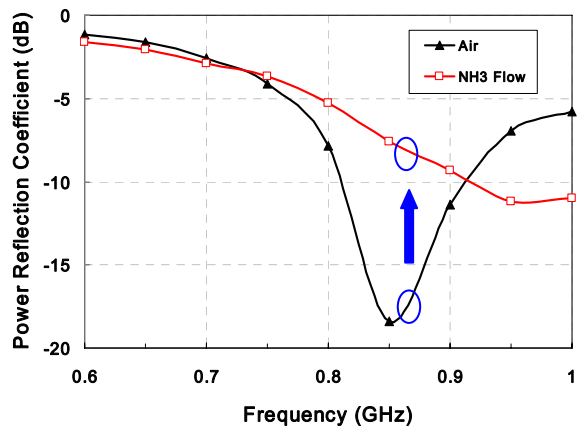


Fig. 8. The calculated power reflection coefficient of the RFID tag antenna with a SWCNT film before and after the gas flow.

A dielectric probe station was used for the impedance measurements. The measured  $Z_{ANT}$  at 868MHz is  $42.6+j11.4\Omega$ . The simulation and measurement results of the return loss of the proposed antenna are shown in Fig. 7, showing a good agreement. The tag bandwidth extends from 810MHz to

890MHz, covering the whole European RFID band. The radiation pattern is recorded as almost omnidirectional at 868MHz with directivity around 2.01dBi and 94.2% radiation efficiency. In order to verify the performance of the conformal antenna, measurements were performed as well by sticking the same tag on a 75mm radius foam cylinder. As shown in Fig. 7, there is almost no frequency shifting observed, with a bandwidth extending from 814MHz to 891MHz. The directivity is slightly decreased to 1.99dBi with 90.3% radiation efficiency. Overall a good performance is still remained with the interested band covered.

In air, the SWCNT film exhibited an impedance of  $51.6-j6.1\Omega$ , which results in a power reflection at -18.4dB. When  $NH_3$  is present, SWCNT film's impedance was shifted to  $97.1-j18.8\Omega$ . The mismatch at the antenna port increased the power reflection to -7.6dB. From (5), there would be 10.8dB increase at the received backscattered power level, as shown in Fig. 8. By detecting this backscattered power difference on the reader's side, the sensing function can be fulfilled.

## CONCLUSIONS

A fully-printed UHF RFID module on paper to form a wireless gas sensor node is presented as a battery-free RFID-enabled sensor solution. To ensure reliable inkjet printing, a SWCNT ink solution has been developed. The impedance performance of the SWCNT film was also characterized up to UHF band. The design demonstrated the great applicability of inkjet-printed CNT for the realization of fully-integrated "green" wireless RFID-enabled flexible sensor nodes based on the ultrasensitive variability of the resistive properties of the CNT materials.

## REFERENCES

- [1] T. Mishima, N. Abe, K. Tanaka, and H. Taki, "Toward construction of a mobile system with long-range RFID sensors" *IEEE conference on Cybernetics and Intelligent Systems*, vol. 2, pp. 960-965, 2004
- [2] M. Philipose, J. Smith, B. Jiang, A. Mamishev, K. Sundara-Rajan, "Battery-free wireless identification and sensing," *IEEE Pervasive Computing*, Volume 4, Issue 1, pp. 37 - 45, 2005.
- [3] S. Johan, Z. Xuezhi, T. Unander, A. Koptyug, H. Nilsson, "Remote Moisture Sensing utilizing Ordinary RFID Tags," *IEEE Sensors 2007*, pp. 308 - 311, 2007
- [4] J.-H. Yun, H. Chang-Soo, J. Kim, J.-W. Song, D.-H. Shin, Y.-G. Park, "Fabrication of Carbon Nanotube Sensor Device by Inkjet Printing", *2008 Proc. of IEEE Nano/Micro Engineered and Molecular Systems*, Jan. 2008, pp. 506-509.
- [5] M. Dragoman, E. Flahaut, D. Dragoman, M. Ahmad, R. Plana, "Writing electronic devices on paper with carbon nanotube ink," *ArXiv-0901.0362*, Jan. 2009.
- [6] L. Yang, R. Zhang, D. Staiculescu, C. P. Wong, and M. M. Tentzeris, "A novel conformal RFID-enabled module utilizing inkjet-printed antennas and carbon nanotubes for gas-detection applications," *IEEE Antennas and Wireless Propagation*, vol. 8, pp. 653-656, 2009.